JOURNAL OF MATERIALS SCIENCE 23 (1988) 3884–3888

Electrical behaviour of CaO-doped ThO_2

VLADIMÍR ŠÁLY, MÁRIA HARTMANOVÁ
Institute of Physics of the Electro-Physical Research Centre, Slovak Academy of Sciences, Bratislava, Czechoslovakia

ALEŠ KOLLER
Research Institute of Electrotechnic Ceramics, Hradec Králové Czechoslovakia

The total a.c. conductivity of a $Ca_xTh_{1-x}O_{2-x}$ solid solution with fluorite-type structure was measured at 1360 Hz with $0 \leqslant x \leqslant 0.25$ and at temperatures of 100 to 600° C. The complex impedance behaviour was investigated at frequencies of 10 to 10^5 Hz and temperatures of 300 to 500° C. The complex dielectric permittivity was calculated at this frequency and in that temperature range. The activation energy for the bulk conductivity was calculated. Its value is about 1.48 eV for $x < 0.03$ and about 1.25 for $x \geqslant 0.03$.

1. Introduction

Among the oxide solid electrolytes, thorium-based materials are important for applications in high temperature galvanic cells, fuel cells, oxygen pumps and sensors. ThO_2-based materials are predominantly oxygen ion conductors over a wide range of temperature and oxygen partial pressure.

The crystal lattice of ThO_2 has a cubic fluorite-type structure. Calcium oxide has a NaCl-type structure [1, 2]. When bi- or tri-valent cations are added to ThO_2, the conductivity of the solution changes.

When thorium is doped with calcium, Ca^{2+} ions replace Th^{4+} ions and electrical neutrality is maintained by the introduction of either oxygen vacancies or Ca^{2+} interstitials. Calcium-doped thorium, as well as most of the oxides with fluorite-type structure, is known as a conductor of O^{2-} vacancies.

The conductivity σ increases when the impurity concentration x increases and vacancies are "free". They begin to associate and create impurity complexes at higher x. The mobility of associated impurities is lower. The conductivity isotherm decreases [3].

Electrical conductivity in calcium-doped thorium electrolytes has been studied [2, 4] but more attention has been paid to yttrium-doped thorium systems [5–7].

The variation of conductivity with temperature gives rise to three regions: the high temperature region, where the conductivity is attributed to dissociated vacancies; an intermediate temperature range where associated vacancy-impurity complexes dominate and a low temperature region where grain boundary effects appear to be significant [4].

The electrical conductivity is usually investigated as a function of temperature T, frequency f and oxygen partial pressure and the activation energy E for the movement of charge carriers is calculated by solving the known equation

$$\sigma T \approx A \exp(-E/kT) \quad (1)$$

where A is the pre-exponential factor and k is the Boltzmann constant.

A lot of results have been published for the complex impedance of zirconium [8, 9] but fewer for thorium-based electrolytes. The complex impedance of yttrium-doped thorium electrochemical cells have been examined by Schouler *et al.* [10].

The study of frequency dependences and complex impedance behaviour can show some new aspects of CaO-doped ThO_2 in cells

$$O_2 \quad Pt\ (x\text{CaO} - (1 - x)\text{ThO}_2)\text{Pt} \quad O_2$$

where $0 \leqslant x \leqslant 0.25$.

In a previous study [2, 4] the total conductivity of CaO-doped ThO_2 was measured at a frequency of 1000 Hz and activation energies were found to be between 0.96 and 1.05 eV below 600° C [4]. The CaO content varied from 0 to 7 mol % and the partial pressure of oxygen was $p_{O_2} = 10^{-23}$ atm. As these results were obtained from measurements at only one a.c. frequency, it is not possible to know more about the separate relaxation processes.

2. Specimen characterization

The investigated samples were all polycrystalline phases. The calcium-doped samples were prepared by sintering of decarbonated, homogenized and compressed pellets at 1825 K for 2 h. The reactants ThO_2 and $CaCO_3$ were both of analytical reagent purity. The pellets obtained were approximately 5 mm in diameter and 1.2 mm thick.

The densities of CaO-doped ThO_2 were measured on a modified Amsler apparatus constructed on the principle of uplift of samples immersed in mercury. The theoretical densities were calculated. The measured densities were in the range from $7.24 \times 10^6\,g\,m^{-3}$ (pure thorium) to $9.03 \times 10^6\,g\,m^{-3}$ ($x = 0.02$) and the calculated densities in the range from $8.61 \times 10^6\,g\,m^{-3}$ ($x = 0.20$) to $9.93 \times 10^6\,g\,m^{-3}$ (pure thorium). The measured lattice parameter a was in all cases 0.559 nm [11].

0022–2461/88 $03.00 + .12 © *1988 Chapman and Hall Ltd.*

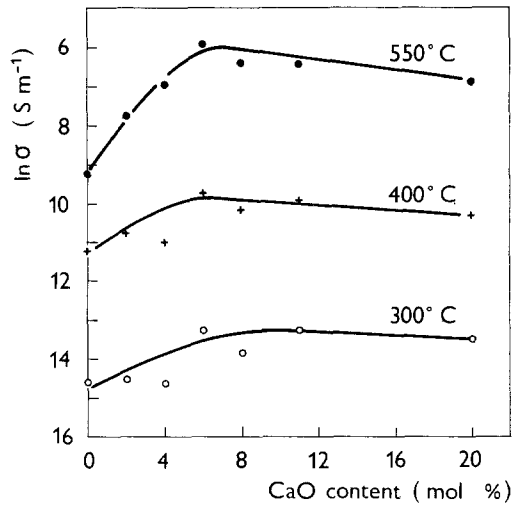

Figure 1 The a.c. conductivity isotherms for ThO_2–CaO solid solution in air, $f = 1360$ Hz.

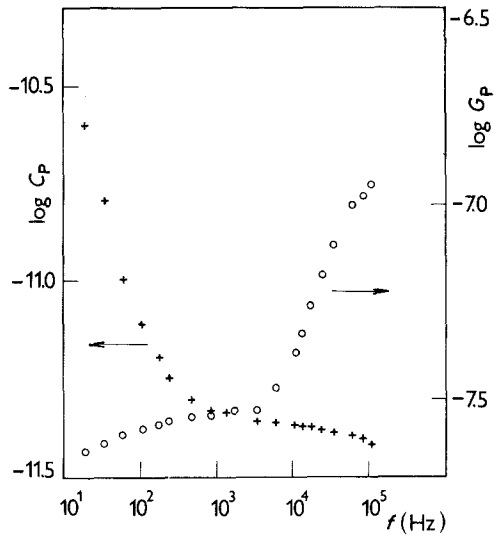

Figure 2 Plots of logarithm of parallel capacitance and conductance against logarithm of frequency at the temperature 301° C, $x = 0.03$.

3. Experimental Procedure

The prepared pellets were painted with platinum emulsion on both sides and heated for 3 h at 1050° C. The process of painting and heating was repeated until the resistance of the electrode was small enough (1 Ω on the diameter of the electrode). The sample was placed into a sample holder with two opposite platinum foil electrodes (10 × 10 mm) pressed against the sample to have a good electrical contact. The measured signal was led by platinum wires.

Capacity and electrical conductivity were measured at temperatures between 100 and 600° C and the frequencies ranged from 10 to 10^5 Hz in air using General Radio Capacitance Bridge 1616. Measurements were performed at an applied a.c. voltage of 5 V. The temperature was controlled by a Chinotherm 10 A (Hungary) and kept constant with an accuracy of ± 0.5° C. The resistance of the leads was neglected. The end of the Pt–Pt10% Rh thermocouple was placed as near as possible to the sample. The complex impedance was calculated for temperatures from 300 to 500° C.

4. Results

4.1. Conductivity

The a.c. total conductivity of pure ThO_2 and CaO-doped ThO_2 (the CaO content varies from 0 to 25 mol %) was measured at temperatures from 100 to 600° C in air. The frequency of the measuring signal was 1360 Hz (an accidental value). The $\ln\sigma$ against CaO content plots at constant temperature pass through a flat maximum at higher temperatures. The maximum was found at about 6 mol % CaO. The effect of the increasing content of CaO on the conductivity was insignificant in samples containing more than 8 mol % CaO. The $\ln\sigma$ against CaO content plots at various temperatures are shown in Fig. 1. The measured parallel conductance and capacitance are plotted against frequency on a logarithmic scale (Fig. 2).

4.2. Complex impedance

Three arcs can be seen on the complex impedance plot of polycrystalline yttrium-stabilized zirconium at 300° C [12]. The situation in the case of CaO-doped ThO_2 is different. The arcs overlap and are deformed. Only one distinct arc is observable for our conditions at higher frequencies and lower temperatures, similar to that shown by Raistrick *et al.* [13]. This arc can be caused by bulk conductivity. The impedance plot in the low frequency part does not have the simple form (Figs 3 and 4) of an arc.

An evident change of the complex impedance plot is observable between 2 and 3 mol % CaO in the low frequency part. The noticeable parameters of the arc (an evident semicircle) depend on the CaO content. We can deduce that this arc characterizes the bulk properties of the ionic conductor. The interfacial phenomena on the electrodes or grain boundaries give rise to the other arc or to the depressed part of the complex impedance plot.

The impedance Z_2 (Figs 3 and 4) is thermally activated and an Arrhenius graph can be constructed (Fig. 5) showing a straight line in the investigated range of 300 to 500° C. Results shown in Fig. 5 were

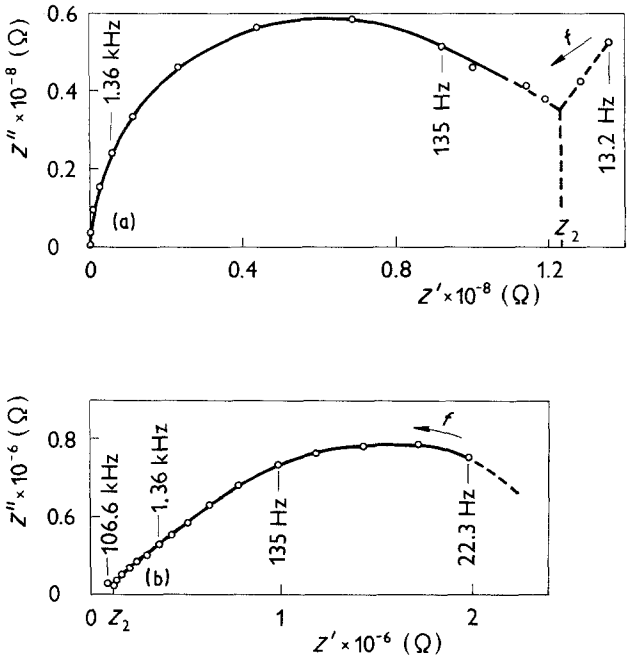

Figure 3 The complex impedance plots obtained at (a) 300° C, (b) 481° C, $x = 0.01$.

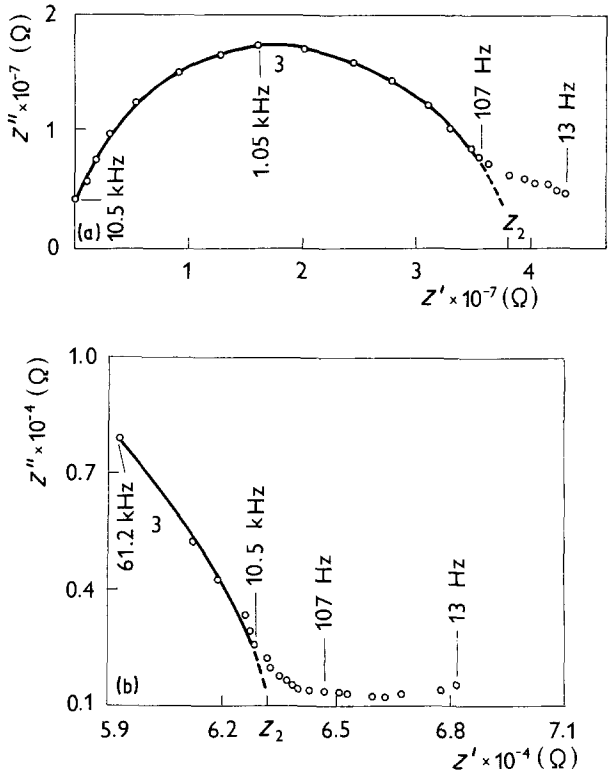

Figure 4 An example of the complex impedance diagram measured at (a) 300° C, (b) 500° C, $x = 0.03$.

calculated by the least squares method. We have calculated the activation energies E of $1/Z_2$ for various contents of CaO in ThO_2. They are presented in Table I. The activation energy of $1/Z_2$ increases when the concentration decreases from 3 to 2 mol % CaO. The low frequency part of the impedance plot is not suitable for evaluation. When the painting and heating of platinum electrodes was repeated, the shape of this part of impedance plot was changed (the slope of curve was changed). This fact is evidently caused by a change in the blocking behaviour of platinum electrodes. The fundamental difference between the low frequency parts of the impedance plots of $x \leqslant 0.02$ and $x > 0.02$ solid solutions was not changed.

4.3. Dielectric permittivity

The complex dielectric permittivity has been calculated from the measured values of capacitance and conductance and its frequency dependence has been plotted. The frequency dependence of the complex dielectric permittivity is thermally activated. The plots are simply shifted with temperature (i.e., the curves keep the same shape) at lower temperatures but not at higher ones. This indicates one relaxation process at lower temperatures [14]. The frequency dependence of the complex dielectric permittivity shown in Fig. 6 has the classical form of ionic conductors with hopping charges [14]. The real part of dielectric permittivity is at a temperature above 100° C and at high frequencies about 23. It increases when the frequency decreases.

TABLE I The activation energies calculated from shifting of the complex impedance diagram

mol % CaO	1	2	3	6	8
Activation Energy (eV)	1.49	1.47	1.26	1.25	1.16

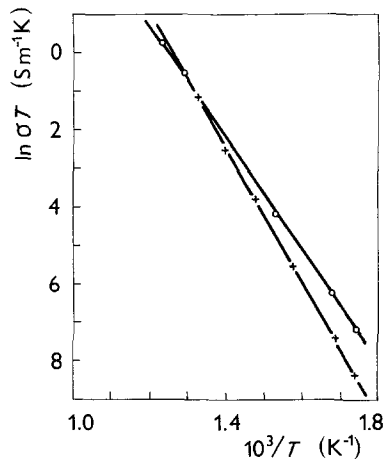

Figure 5 The Arrhenius diagram of the bulk conductivity determined by the complex impedance method, $x = 0.01$ (+) and 0.03 (○).

5. Discussion

In a ThO_2–CaO solid solution, substitution of Th^{4+} ions by Ca^{2+} ions results in an overall charge of -2 per impurity cation site. The total conductivity σ of a substance may be expressed by

$$\sigma = \sum_i n_i q_i \mu_i = \sum_i \sigma_i \qquad (2)$$

where n_i is the number of carriers per unit volume, q_i is the charge of the carrier and μ_i is its mobility. So that σ_i is the partial conductivity. Details about ionic conductivity are available in references [15–17].

In order to explain the dependence of ionic conductivity on the impurity content, Subbarao and Ramakrishnan [16] suggested a model in which the neighbours of a vacancy are taken into account. A vacancy is completely free if its nearest neighbours are all Th^{4+} ions, its mobility $\mu = \mu_1$. If the number of nearest neighbours around a vacant site is z_1, $(1 - x)^{z_1}$ is the probability that the nearest neighbours are Th^{4+} ions. Then for the concentration x at the maximum of the conductivity plot it follows that

$$x_{max} = \frac{1}{z_1 + 1} \qquad (3)$$

σ is reduced if there are no oxygen ions in the negative ion sites to which the vacancy can jump. The vacancy correlations have yet to be considered. The number of free vacancies increases with respect to the fact that the vacancy mobility is not strictly zero if there is a

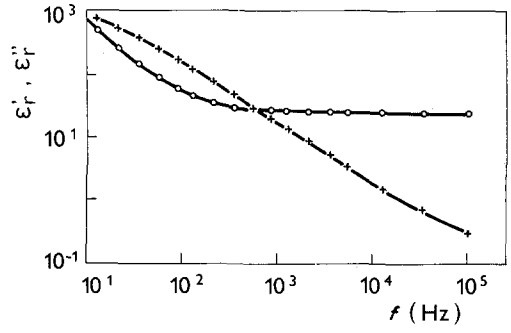

Figure 6 The frequency dependence of complex dielectric permittivity at 320° C, $x = 0.01$. (○ ε'_r, + ε''_r).

Ca^{2+} nearest neighbour. An additional factor, which can limit the conductivity of the ionic conductor, is the formation of an ordered crystalline phase. No interstitial solid solution was found in the CaO–ThO_2 system for $x \leqslant 0.4$ but a small number of Ca^{2+} ions enter the interstitial position [11]. They can create clusters and affect the conductivity.

The maximum of the conductivity isotherm becomes clear at the higher temperatures. Mostly electrons (or holes) take part in the conductivity process at the lower temperatures [18] in air. That means, the ideas about isothermal behaviour of ionic conductivity shown in references [11, 16] need not be strictly valid in our case.

The complex impedance or admittance behaviour of ionic conductors was studied by Bauerle [19] and Wang and Nowick [20]. Three distinct arcs are generally observed. At higher temperatures there appears an arc which has its origin in the electrode polarization effects. The second and the third arcs are related to the behaviour of the polycrystalline electrolyte itself.

No such evident behaviour was observed for thorium-based electrolytes, Y_2O_3-doped ThO_2 [10] and CaO-doped ThO_2. Grain boundary and electrode polarization effects are not separable in the complex impedance plot of calcium-doped thorium.

With x higher than 0.02 no arc due to polarization effects on the electrode–electrolyte boundary appeared below 600° C under our experimental conditions. It is possible that this part will be better marked at higher temperatures. (The specimens are too conductive to be measured above 600° C on the General Radio Bridge 1616). In our opinion, at the higher x more Ca^{2+} ions enter the interstitial position and create defects with various magnitude and relaxation times which affect the shape of the impedance plot (Figs 3 and 4).

Discussions concerning an equivalent circuit and circuit elements which describe complex impedance behaviour are given in references [13, 21, 22].

The bulk conductivity $1/Z_2$ of calcium-doped thorium was found to be activated with energies presented in Table I. The activation energy of the bulk conductivity does not depend on the CaO content within the measurement and calculation accuracies at the two intervals $-x < 0.03$ and $x \geqslant 0.03$. The shape of the complex impedance plot also changes on the boundary of these intervals.

The complex dielectric permittivity against frequency plot is only shifted with temperature at lower temperatures. The shape of the plot is the same after the change of temperature. This does not hold at higher temperatures when the shape of the curve changes as well. The frequency at the point of the cross-section in Fig. 6 is shifted with temperature with the activation energy E. For example when $x = 0.01$, the activation energy calculated from the $1/Z_2$ activation and the dielectric permittivity plots activation 1.49 and 1.42 eV, respectively, are in good agreement. We can suppose the activation energy calculated at lower temperatures from the dielectric permittivity activation, when the shape of plot does not change, is the activation energy of the bulk conductivity at low temperatures and high frequencies.

The complex impedance plots (Figs 3a and 4a) can be approximated by circles with centres displaced below the real axis. Such behaviour of polycrystalline ionic conductors was described by Raistrick *et al.* [13, 21]. They proposed a circuit of parallel conductance, resistance and constant phase element to account for the complete bulk frequency response. This case is said to be caused by distribution of relaxation times. In such a way a plot of log G_p against log f should be a straight line. As it can be seen from Fig. 2 this condition is fulfilled only at two orders of magnitude of intermediate frequencies of the high frequency part. Therefore we believe that a better approximation of this situation is the Debye–Hückel-type relaxation as proposed in a model of Funke [23]. This model considers the shortest and longest relaxation times existing in real systems. Therefore the arc should deviate from the circular shape in the limits of low and high frequencies. Simultaneously the plot of log G_p against log f also deviates from a straight line.

6. Conclusion

In the system CaO–ThO_2, the CaO content affects both, the total a.c. conductivity and the bulk conductivity. (The bulk conductivity is a part of the total a.c. conductivity).

The shape of the complex impedance plot for $x \geqslant 0.03$ changes when $0 \leqslant x \leqslant 0.25$. The change may be due to the creation of the complex defects at this impurity concentration.

The dependences of the complex dielectric permittivity on frequency are shifted with temperature to higher frequencies. The activation energy calculated from the complex dielectric permittivity at lower temperatures and the complex impedance plots are comparable and may characterize the bulk conductivity.

References

1. H. H. MOEBIUS, *Z. Chem.* **4** (1964) 81.
2. A. K. MEHROTRA, H. S. MAITI and E. C. SUBBARAO, *Mater. Res. Bull.* **8** (1973) 899.
3. F. HANIC, M. HARTMANOVÁ, M. PROKEŠOVÁ and A. KOLLER, Proceeding 7th konference čs. fyziku, Praha (Jednota ČS. matematiku a fyziku-Fyzikálni vědecka sekce, Praha, 1981) p. 6.
4. H. S. MAITI and E. C. SUBBARAO, *J. Electrochem. Soc.* **123** (1976) 123.
5. E. C. SUBBARAO, P. H. SUTTER and J. HRIZO, *J. Amer. Ceram. Soc.* **48** (1965) 443.
6. J. M. WIMMER, L. R. BIDWELL and N. M. TALLAN, *ibid.* **50** (1967) 198.
7. R. E. W. CASSELTON, *Phys. Status Solidi (a)* **3** (1970) K 255.
8. M. KUWABARA, T. MURAKAMI, M. ASHIZUKA, Y. KUBOTA and T. TSUKIDATE, *J. Mater. Sci. Lett.* **4** (1985) 467.
9. S. IKEDA, O. SAKURAI, K. UEMATSU, N. MIZUTANI and M. KATO, *J. Mater. Sci.* **20** (1985) 4593.
10. E. SCHOULER, A. HAMMOU and M. KLEITZ, *Mater. Res. Bull.* **11** (1976) 1137.
11. F. HANIC, M. HARTMANOVÁ and S. KRCHO, *Solid State Ionics* (in press).
12. S. P. S. BADWALL and M. V. SWAIN, *J. Mater. Sci. Lett.* **4** (1985) 487.
13. I. D. RAISTRICK, CH. HO and R. A. HUGGINS, *J. Electrochem. Soc.* **123** (1976) 1469.

14. A. K. JONSCHER, "The Universal Dielectric Response – a Review of Data and Their New Interpretation", Academic, London (1980).
15. M. F. LASKER and A. R. RAPP, *Z. Phys. Chem. N.F.* **49** (1966) 198.
16. E. C. SUBBARAO and T. V. RAMAKRISHNAN, Proceedings Fast Ion Transport in Solids, Electrodes and Electrolytes, Wisconsin, (1979) edited by P. Vashishta, J. N. Mundy and G. K. Shenoy, (Elsevier, New York, 1979) p. 653.
17. K. D. HOHNKE, *ibid.*, 669.
18. H. S. MAITI and E. C. SUBBARAO, *J. Electrochem. Soc.* **123** (1976) 1057.
19. J. E. BAUERLE, *J. Phys. Chem. Solids* **30** (1969) 2657.
20. D. Y. WANG and A. S. NOWICK, *J. Solid State Chem.* **35** (1980) 325.
21. I. D. RAISTRICK, *Solid State Ionics* **18 & 19** (1986) 40.
22. R. L. HURT and J. R. MACDONALD, *ibid.* **20** (1986) 111.
23. K. FUNKE, *ibid.* **18 & 19** (1986) 183.

Received 16 July 1987
and accepted 28 April 1988